UDK 620.178.16:669.1.017:67.017
Original scientific article/Izvirni znanstveni članek

ISSN 1580-2949
MTAEC9, 55(6)753(2021)

EFFECT OF DIFFRENT LOADS ON THE WEAR BEHAVIORS OF 5Cr5Mo2V STEEL AT 700 °C

VPLIV RAZLIČNIH OBREMENITEV NA OBRABO JEKLA 5Cr5Mo2V PRI 700 °C

Zhixiong Bai, Hang Yang, Ning Su, Xiaochun Wu*

School of Materials Science and Engineering, Shanghai University, Shanghai 200072, China

Prejem rokopisa – received: 2021-07-23; sprejem za objavo – accepted for publication: 2021-08-30

doi:10.17222/mit.2021.222

The effect of different loads on the high-temperature wear behavior of 5Cr5Mo2V steel at 700 °C was investigated. Wear morphologies, oxide compositions and matrix evolution were studied. The results showed that the wear rate increased with an increased test load, and the wear mechanism transformed from abrasive-oxidative wear to adhesive-oxidative wear. The relation between a delaminated oxide layer and cracks in the matrix were investigated. The exfoliation of carbides and displacement difference between the matrix and carbides caused a crack initiation. The wear rate strongly related to carbides, and coarse M_6C carbides with poor holding power led to a high wear rate. Besides, a diagram of wear characteristics under different loads was suggested in this work.

Keywords: load, wear mechanism, oxide, diagram

Avtorji so v članku raziskovali vpliv različnih obremenitev na visoko-temperaturno obrabo jekla vrste 5Cr5Mo2V pri 700 °C. Pri tem so študirali morfologijo obrabe, sestavo oksida in razvoj kovinske matrice. Rezultati raziskave so pokazali, da hitrost obrabe narašča z naraščajočo obremenitvijo, mehanizem obrabe pa se pretvori iz abrazivno-oksidativnega v adhezivno-oksidativnega. Ugotavljali so tudi, kakšna je povezava med cepljenjem oksidne plasti in nastalimi razpokami v matrici. Nastajanje razpok je povzročilo izluščenje karbidov iz matrice ter razlike v premikih med matrico in karbidi. Hitrost obrabe je bila močno povezana z obliko in velikostjo karbidov. Večjo hitrost obrabe so povzročali grobi M_6C karbidi s slabšo vpetostjo v matrico. Avtorji svetujejo uporabo karakterističnega diagrama obrabe v odvisnosti od uporabljene obremenitve.

Ključne besede: obremenitev, mehanizem obrabe, oksid, diagram

1 INTRODUCTION

With the development of the automotive industry, hot stamping dies play an increasingly important role. At high-temperature conditions, a hot stamping die is kept in service with strong pressure and friction, which are likely to cause wear failure.[1–3] According to statistics, the wear failure of hot stamping dies accounts for about 70 % of failure behaviors.[4] Therefore, the wear failure of hot stamping die steel has received more and more attention. According to researches, there are different wear mechanisms in different temperature environments. Wei et al.[5] found that as a load increased from 50 N to 250 N, the wear mechanism of H13 and H21 steel transformed from mild oxidation wear to severe wear at 400 °C. The wear characteristics of H13 steel transformed from adhesive wear to oxidative mild wear at 20–200 °C.[6] During wear, different microstructures of steel play a significant role in the wear rate. Li et al.[7] found that the cementite breakage of upper bainite caused an increase in the wear rate when compared with pearlite. For Ni–Cr–Mo–V steel, Rai et al. studied the wear behavior of different microstructures and found that a microstructure with higher yield strength and hardness showed a higher transition load.[8] Regarding the high-temperature wear resistance, scholars usually pay attention to the connection between wear characteristics and the matrix. Li et al.[9] proposed that the wear resistance of steel could be improved at a high temperature by adding tungsten and molybdenum. The unstable secondary carbides, precipitated along the boundaries of grains and laths resulted in severe wear.[10]

Li et al.[11] found that Mo_2C and VC carbides could keep the high-temperature hardness of a matrix, delaying the transition from mild wear to severe wear. Hashemi et al.[12] suggested that the wear resistance of V-rich MC carbides was better than that of W-rich M_2C carbides. The great bearing capacity of coarse MC carbides could form a stable oxide layer on a worn surface to resist wear.[13] Besides, an oxide layer could increase the holding power of a matrix, preventing large deformation.[14] Therefore, a stable oxide layer is essential for the reduction of wear, especially at a high temperature. On the basis of some studies, the oxide formation is affected by the wear speed, temperature, alloy elements and so on. Jayashree et al.[15] stated that a high flash temperature promotes the formation of a compacted oxide layer during sliding. Tang et al.[16] showed that a high content of anti-oxidation elements could form a more compact oxide layer during wear. Fontalvo et al.[17] stated that the content of alumi-

*Corresponding author's e-mail:
380959525@qq.com (Xiaochun Wu)

num and silicon led to a reduced thickness of the oxide layer. However, others found some special factors that result in the delamination behavior of the oxide layer at a high temperature. Wang et al.[18] thought that the delamination of the oxide layer easily occurred under high-speed sliding. Shi et al.[19] indicated that coarse M_6C carbides caused delamination of the oxide layer and proposed a new schematic diagram of the oxidation wear of DM steel.

According to the above studies, microstructures, carbides, alloy elements and oxides strongly affect the wear resistance at high temperature. Unfortunately, these researches seem not to clarify the relationship between loads, carbides, oxides and wear mechanisms. The goals of this work were to describe the wear characteristics of a novel hot stamping steel under different loads and the formation mechanism of the delaminated oxide layer.

2 EXPERIMENTAL PART

5Cr5Mo2V is a new hot stamping steel; its chemical composition is shown in **Table 1**. 5Cr5Mo2V steel was held for 30 min at 1060 °C to be austenitized, subsequently quenched in oil, finally held for 2 h at 520 °C and 560 °C for tempering, respectively. The microstructures of 5Cr5Mo2V steel were transformed into tempered martensite with heat treatment; the hardness was (55 ± 0.4) HRC (about 605 HV). **Figure 1** shows the microstructure of 5Cr5Mo2V steel; the matrix was martensite with fine carbides after tempering. According to the simulation results of Jmat-Pro, the types of carbides were M_2C and $M_{23}C_6$ and their contents were 0.4 *w*/% and 6.08 *w*/%, respectively. Before the wear test, samples were cleaned with ethanol and their roughness was about 0.25 μm.

Table 1: Chemical compositions of 5Cr5Mo2V steel (*w*/%)

Steel	C	Si	Mn	Cr	Mo	V	P	S
5Cr5Mo2V	0.49	0.15	0.39	4.79	2.22	0.54	0.016	0.0010

Wear tests were performed on a reciprocating ball-on-disk high-temperature wear instrument (UMT-3 type, America). The ball (ϕ 9.5 mm, HV 2800) consisted of SiC ceramic, which has good thermal stability at high temperatures. The wear samples were fixed onto the base and tested at 700 °C and a sliding frequency of 5 Hz.

The sliding speed was 50 mm/s and the total sliding distance was 360 m. The test loads were (10, 15, 20, 25 and 30) N. Three samples were tested at the same condition to ensure the reliability of the tests. The wear volume was measured with a Contour white-light interferometer (GT-K type, America) and the wear rate was calculated based on Equation (1):

$$W_s = \frac{V}{(P \times L)} \quad (1)$$

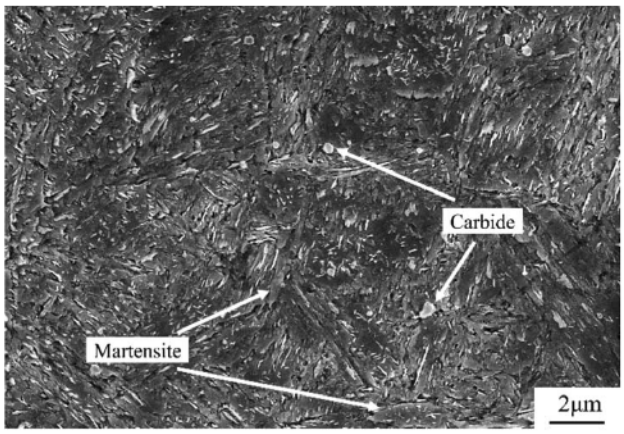

Figure 1: Microstructure of 5Cr5Mo2V steel

where V is the wear volume (mm^3); P is the pressure (N); L is the sliding distance (m). The microstructures and morphologies of the worn surfaces were analyzed using a scanning electron microscope (SEM, Supra-40 type, Germany). The types and amounts of oxides on the worn surfaces were analyzed with X-ray diffraction (XRD, D/MAX-2500 type, Japan); the scanning range was 20–80° and the velocity was 4 °/min. The Vickers hardness distribution from the surface to the substrate was measured using a digital microhardness tester (UM-3 type, China) with a load of 500 g and dwell time of 10 s. The Vickers hardness was examined at five different positions of each sample. The microstructures of steel were identified with a transmission electron microscope (TEM, JEM-2010F type, Japan) and the accelerating voltage was 20×10^5 V.

3 RESULTS

The morphologies of the worn surfaces of 5Cr5Mo2V steel under different loads are presented in **Figure 2**. A large number of oxide particles were observed on the worn surface under an experimental load of 10 N, as shown in **Figure 2a**. The contact surface of the oxide layer fractured, and spalling regions were parallel to the sliding direction. **Figure 2b** shows the morphology of the worn surface under 15 N; smooth zones appeared on the worn surface. A large number of oxide particles were compacted by the pressure and friction during dry-sliding wear, and the worn surface gradually formed a complete oxide layer. Some small pits were formed in the oxide layer. Simultaneously, due to the deformation of oxide layer under the mechanical stress, fatigue cracks were generated gradually. **Figure 2c** shows that the worn surface of 5Cr5Mo2V steel was entirely covered with an oxide layer under 20 N. In addition, grooves appeared on the surface with the plastic deformation of the matrix. When the load reached 25 N, the worn morphology of 5Cr5Mo2V steel changed compared with that formed under 20 N, as seen in **Figure 2d**. According to the worn morphology, a lot of adherent ox-

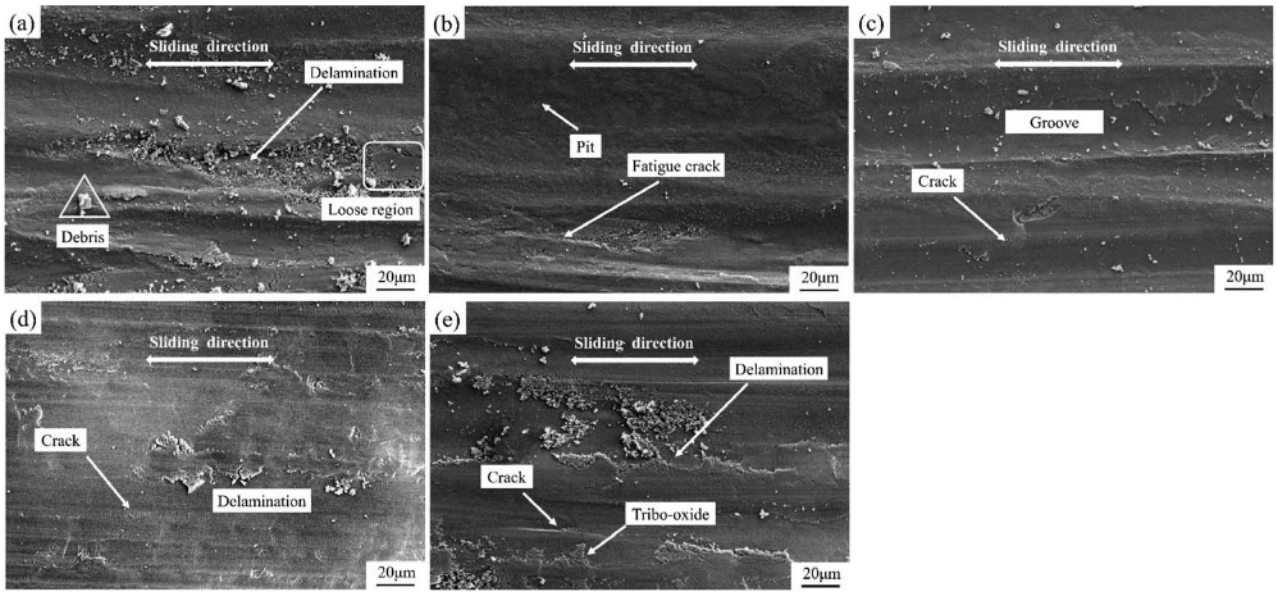

Figure 2: Worn-surface morphology of 5Cr5Mo2V steel: a) 10 N, b) 15 N, c) 20 N, d) 25 N, e) 30 N

ides that could resist the wear were observed on the worn surface, the new oxide particles were compacted on the formed oxide layer and an obvious delamination was found at the oxide surface. In the meanwhile, cracks perpendicular to the sliding direction were found on the worn surface, which was a sign of the peeling of oxides. The oxides repeated the cycle mechanism of compaction and peeling during high-temperature wear. **Figure 2e** shows that the compacted oxide layer was relatively looser as compared with that under 25 N. Loading and unloading of the contact zone cause fatigue cracks during reciprocating sliding. It is worth emphasizing that cracks expanded under the pressure and ultimately caused oxides to peel off. Also, due to pressure and friction, the edge of the recompacted oxide layer cracked and lost its adhesion.

According to the XRD analysis of the oxides on the worn surface, the composition of oxides included FeO, Fe_2O_3 and Fe_3O_4 under different loads, and the amount of oxides increased with the increasing test load, as shown in **Figure 3**. Pressure could affect the activity of the components in the metal and the oxidation rate of the metal surface. In order to study the mechanism, researchers proposed "thermodynamic activity".[20] The mathematical expression of the thermodynamic activity is shown with Equation (2):

$$a_i' = a_i \cdot \exp\left[\frac{n_i \Delta p V}{RT}\right] \quad (2)$$

Where a_i' is the thermodynamic activity of component i under pressure; α_i is the static thermodynamic activity of component i; Δp is the pressure difference; V is the molar volume of metal; n_i is the quantity fraction of component i; R is the gas constant; T is the thermodynamic temperature. It can be seen that a_i' and Δp are positively correlated, and the thermodynamic activity and the oxidation rate increase with an increase in the pressure. The theory is consistent with the experimental result. The mechanism of the surface oxidation behavior can be analyzed from two aspects: high-temperature oxidation thermodynamics and high-temperature oxidation kinetics. In the initial stage of oxidation, the surface oxidation rate was affected by a chemical reaction. When the oxide layer was formed on the surface, the growth of the oxide layer was affected by the diffusion of the elements in the oxide layer. During the early wear, more vacancies and dislocations promoted the nucleation of oxides on the surface under pressure.[21] The formation of oxides increased the grain boundary volume, which promoted the short-path diffusion of elements. Therefore, the oxidation rate was significantly accelerated. Besides, pressure also promoted the short-path diffusion of elements and increased the oxidation rate. In the mean-

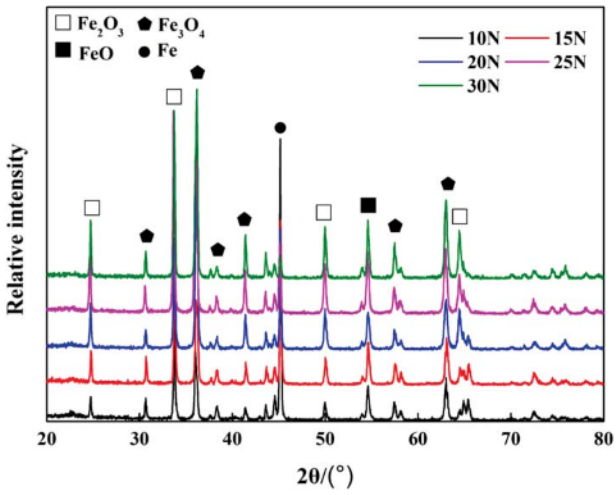

Figure 3: XRD spectrum analysis of the surface of 5Cr5Mo2V steel after wear

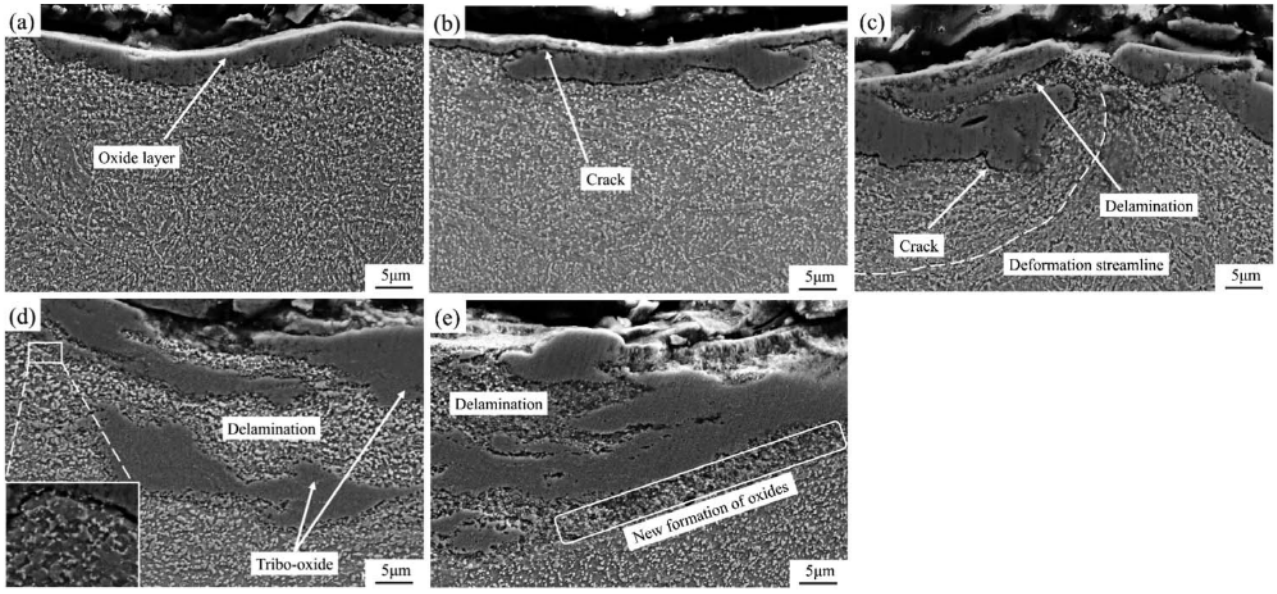

Figure 4: Worn cross-sectional morphology of 5Cr5Mo2V steel: a) 10 N, b) 15 N, c) 20 N, d) 25 N, e) 30 N

while, the oxide layer was easier to deform, crack and peel off under pressure to reveal the "fresh surface". The "fresh surface" with its high reactive energy accelerated the growth of oxides.

Figure 4 shows the cross-sectional wear morphologies of 5Cr5Mo2V steel under (10, 15, 20, 25 and 30) N. In **Figure 4a**, it can be seen that the worn surface was completely covered with an uneven oxide layer with a thickness of 3 μm, effectively hindering a direct contact between the SiC ceramic ball and the matrix. In addition, the oxide layer was deformed under 10 N and many small cavities were found in the oxide layer, promoting the diffusion of oxygen atoms and accelerating the formation of oxides. When the test load was 15 N, the oxide layer grew irregularly, as shown in **Figure 4b**. Microcracks appeared in the oxide layer and oxygen diffused to the matrix along these cracks, which accelerated oxidation. The delamination of the oxide layer and deformation streamline of martensite are observed in **Figure 4c**. When the load reached 20 N, the matrix produced a plastic flow, and a significant shear force caused cracks in the matrix. In the meanwhile, the loosening of the oxide layer implied that the oxides would separate. Compared with the cross-sectional wear morphology under 20 N, a more obvious delamination of the oxide layer appeared under 25 N, as shown in **Figure 4d**. The formed oxide layer was more compact without obvious cavities. In particular, the carbides near the oxide layer dispersed in the matrix. **Figure 4e** shows the cross-sectional wear morphology of 5Cr5Mo2V under 30 N. The microstructure of the matrix remained similar to that observed under 25 N. This shows that new oxides formed along the oxide layer. The extent of the oxide-layer delamination was more serious.

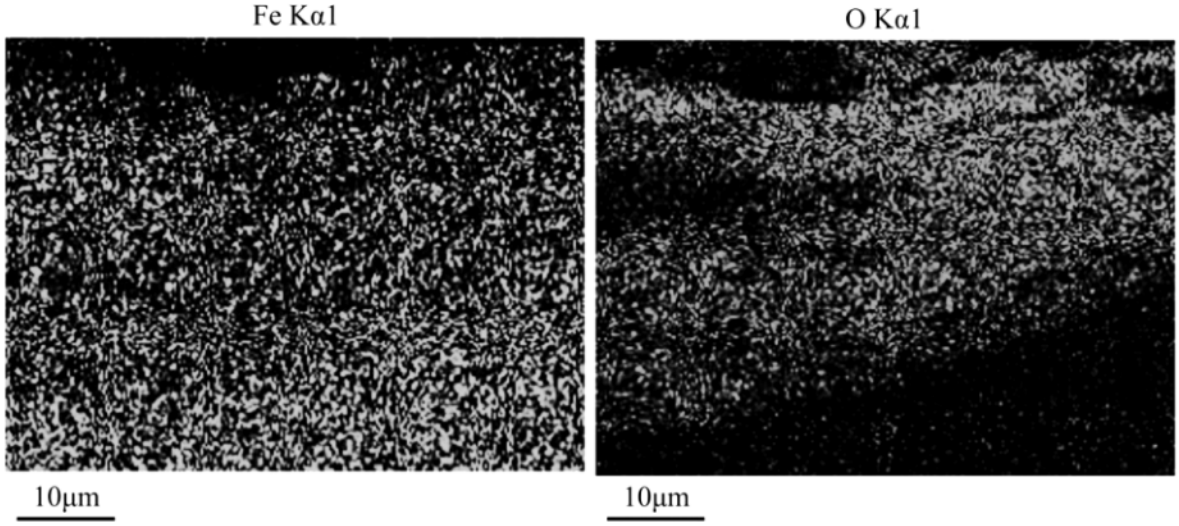

Figure 5: EDS map-scanning analysis of the cross-sectional morphology under 30 N

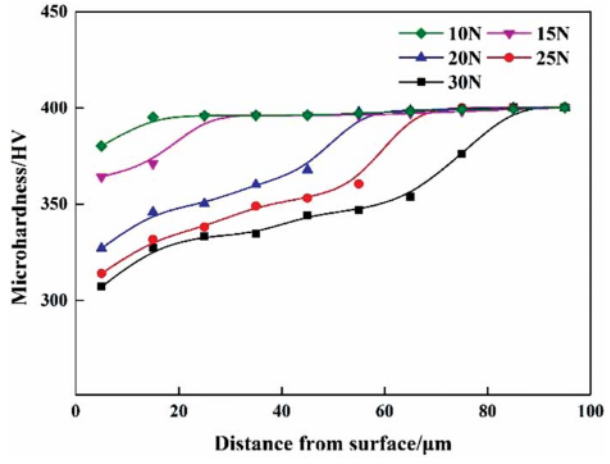

Figure 6: Microhardness distribution on the cross-section of 5Cr5Mo2V steel after wear

Figure 6 shows the microhardness distribution of the cross-section under different loads. The hardness of the matrix was about 400 HV after the wear at 700 °C. Besides, the matrix near the oxide layer had poor hardness and thermal softening appeared in the subsurface. The depth of the softened layer was 15–25 μm under the loads of 10 N and 15 N. During the wear at a high temperature, friction force and pressure caused plastic deformation, dynamic recovery and recrystallization, affecting the softening extent of the matrix. Therefore, when the load reached 25 N and 30 N, a stronger softened layer appeared with a depth of about 70 μm and 90 μm, respectively. Besides, the thermal softened layer of the matrix affected the morphologies of the oxide layer. When the matrix could provide a good support to the oxide layer under a low load, a complete oxide layer appeared. With the increase in the load, the hardness of the softened layer decreased severely, and the oxide layer delaminated without a good support from the matrix.

The evolution of carbides plays a key role in the strength of a matrix. The precipitation and growth of carbides are determined by two basic factors – the supersaturation state of carbide atoms and the diffusion capacity of elements.[22,23] Both of these factors were related to the temperature and deformation of the matrix. The evolution of the microstructure with the increase in the load is illustrated with **Figure 7**. According to the morphologies of the microstructure, a large number of finely dispersed carbides precipitated under deformation and the carbides aggregated and grew with the increase in the load. They showed that the carbon atoms of 5Cr5Mo2V steel had a strong diffusion ability at 700 °C. Besides, deformation produced a large number of dislocations, which provided diffusion channels for the carbon atoms.[24] A long dwell time at the high temperature also provided an advantageous condition for the diffusion of carbon atoms and caused the aggregation and coarsening of carbides.[25] According to **Figure 7b**, carbides grew up under 30 N and the martensite almost disappeared with severe recovery.

The friction coefficient of 5Cr5Mo2V steel under different loads is shown in **Figure 8a**. Under 10 N, although the oxide layer was tightly combined with the matrix, there was a lot of debris as wear particles on the worn surface, causing an increase in the friction coefficient. When the load reached 15 N, run-in and stabilization occurred during the wear. The bumps of the matrix contacted the friction pair, generating great friction at the beginning of dry reciprocating sliding. At the stabilization stage, the bumps disappeared and the contact area increased; a complete oxide layer played a self-lubrication role, gradually decreasing the friction coefficient during the wear. When the load was higher than the critical value, the coarse carbides and severely softened layer caused an increase in the friction coefficient. Therefore, under 20 N and 25 N, the average friction coefficient values of the 5Cr5Mo2V steel were 0.41 and 0.43, respectively. The wear rate of 5Cr5Mo2V under various loads is shown in **Figure 8b**. The oxides on the worn surface partly peeled off, causing abrasive wear under 10 N. When the load was 15 N, the oxide layer was tightly attached to the substrate and the matrix provided a good support for the oxide layer. Therefore, the oxide layer as the protective layer induced a low wear rate. Neverthe-

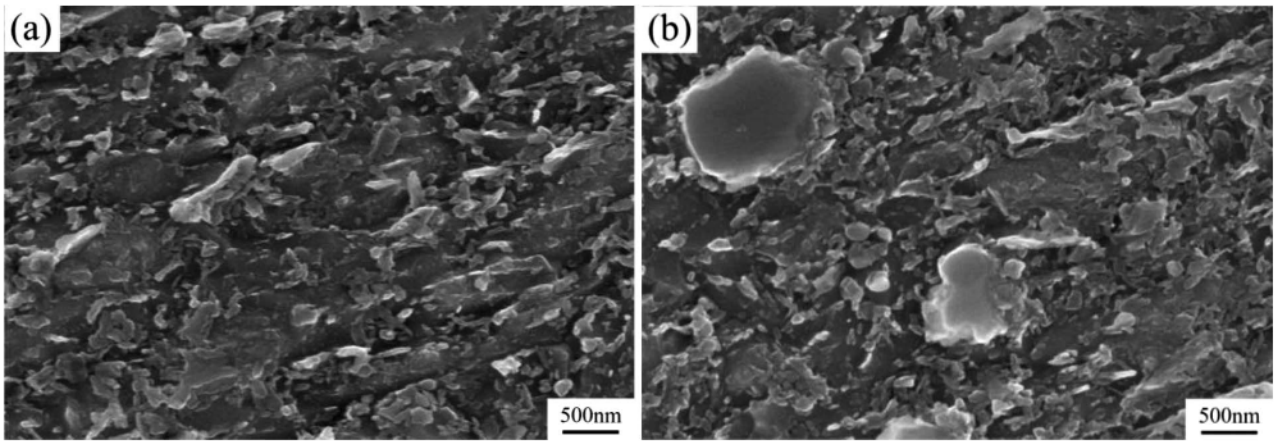

Figure 7: Microstructure of 5Cr5Mo2V steel: a) 10 N, b) 30 N

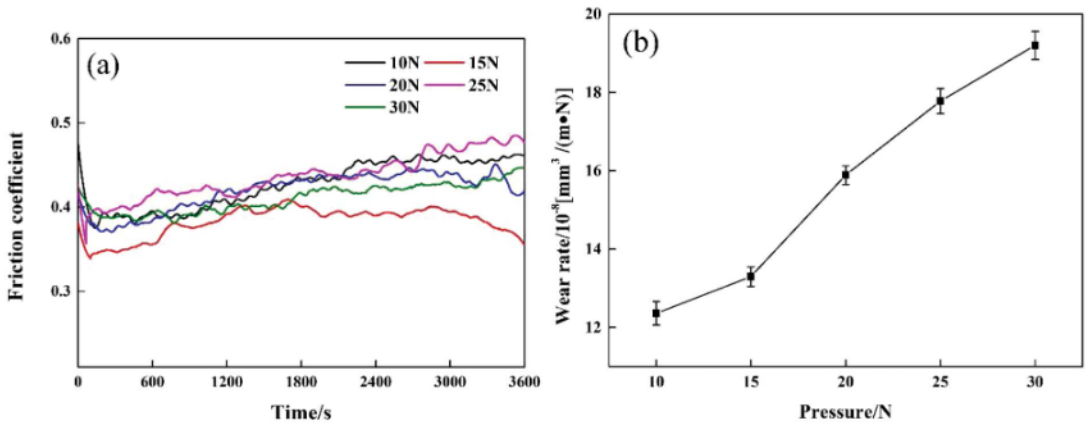

Figure 8: Friction coefficient and wear rate of 5Cr5Mo2V steel: a) friction coefficient, b) wear rate

less, when the matrix was severely softened, the wear rate under 20 N significantly increased to 15.89×10^{-8} mm^{-3}/(m·N). Different morphologies of the oxide layer and carbides caused the wear rate to increase further to 17.78×10^{-8} mm^{-3}/(m·N) under 25 N. These observations suggest that both the hardness of the matrix and morphologies of the oxide layer affected the wear rate.

4 DISCUSSION

The wear of metal materials in a high-temperature and oxidation environment has been widely studied. The stability of carbides at a high temperature has an important influence on the wear resistance. Regarding the wear resistance, carbides play an antiwear-phase role due to their good high-temperature stability. Therefore, in order to illustrate the influence of carbides on the wear characteristics, **Figure 9** shows the type and size of carbides after the heat treatment. **Figure 9a** shows that a large number of dislocations aggregated near lath martensite. M_7C_3-type carbides appeared in the microstructure after the calibration; they were about 110 nm, as shown in **Figure 9b**. According to researches, M_7C_3-type carbides have poor thermal stability and are easily coarsened.[26] **Figures 9c** and **9d** show the TEM morphologies of 5Cr5Mo2V steel with a hardness of 400 HV. According to the analysis of the precipitation phase, there were M_6C-type carbides with a face-centered cubic structure of 170 nm. This means that M_7C_3-type carbides were transformed into M_6C-type carbides at 700 °C. Cui et al.[27] concluded that coarse carbides deteriorate the wear resistance, resulting in the delamination of an oxide layer. Besides, coarse carbides with poor holding power reduce the strength of a matrix. The matrix undergoes a

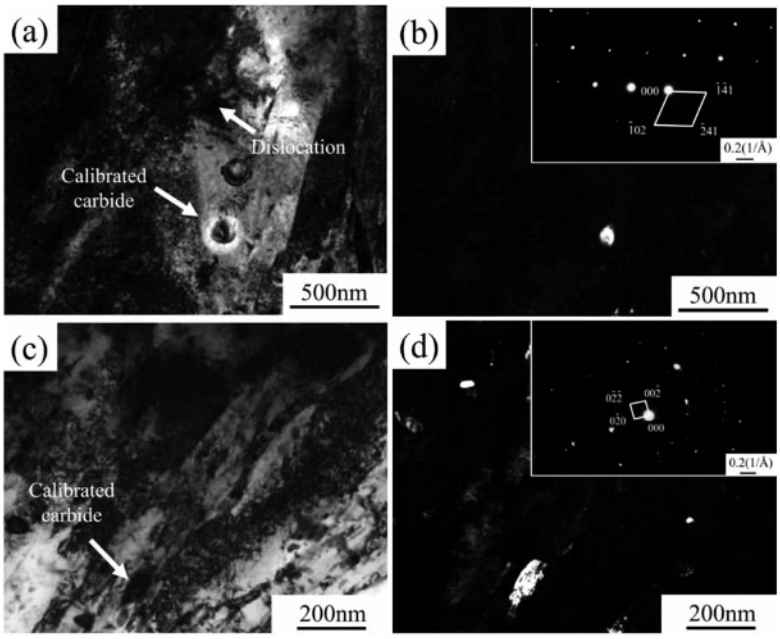

Figure 9: TEM morphology of 5Cr5Mo2V steel: a) bright-field image of M_7C_3 (after heat treatment), b) dark-field image of M_7C_3 (after heat treatment), c) bright-field image of M_6C (400 HV), d) dark-field image of M_6C (400 HV)

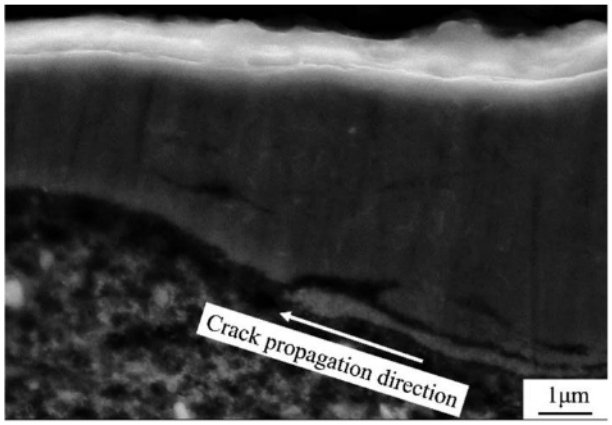

Figure 10: Cracks in the matrix

large plastic deformation under a load, promoting oxidation, and severe oxidative wear occurs.

During wear, the contact between the friction pair and micro-bumps could easily cause defects on the worn surface, which resulted in a stress concentration and fatigue-crack initiation. The varieties of the matrix had a significant impact on the initiation and propagation of cracks. The evolution of the microstructure led to changes in the strength and hardness of the matrix, which directly affected the crack initiation. Besides, the crack initiation and propagation were also closely related to the shear stress. Particularly when crack initiation and propagation were mainly affected by the shear stress, the crack-propagation direction was changing until it was parallel to the shear direction.[28] In this work, a similar result was also observed. The direction of the matrix cracks near the oxide layer was the same as the sliding direction, as shown in **Figure 10**. In addition, with the diffusion of oxygen atoms, oxidation gradually occurred in the cracks.

With the increase in the load, more cracks are initiated and propagated. Eventually, this leads to the delamination of the oxide layer with the oxidation. In order to explain the delamination of the oxide layer, it is necessary to explore the reason for the crack formation in the matrix. The formation of matrix cracks can be divided into four steps during early wear, as shown in **Figure 11**. Firstly, the size of carbides does not changed significantly. Then, carbides coarsen and become hard and large particles in the second stage. As the wear depth increases, carbides have a direct contact with the friction pair and are subjected to the press and tensile forces. As carbides are rigid spheres, when the tensile stress surpasses the binding force at the interface between the matrix and carbides, carbides peel off and small cracks appear, as illustrated in the fourth stage. Besides, the matrix is prone to plastic deformation at a high temperature and load. If the dimension of carbides and stress surpass the critical values, a displacement difference between the matrix and coarse carbides occurs and cracks are initiated.[29–30] So, in two cases, cracks appear in the matrix with the accumulation and release of stress. Furthermore, when oxygen atoms enter the cracks and form oxides, oxides with a low Young's modulus and high thermal-expansion coefficient cause a stress concentration, accelerating the growth of the cracks.

Both the oxide layer and microstructure of the matrix markedly affect the oxidative wear characteristics and mechanisms. Although all test samples were subjected to oxidative wear, the morphologies of the oxide layer were different, and the wear mechanism of the samples was a combination of different types in particular situations. The oxidative-wear theory by Quinn[31–33] says that the oxide layer with mild wear and a low pressure can sufficiently grow until its thickness reaches the critical thickness, and then it starts to peel off. In this case, the wear rate is only determined by the oxide layer, while the matrix and load play a small role. Due to the high temperature and load in this work, the wear mechanism is different from Quinn's oxidative wear. When the matrix provides good support to the oxide layer, the oxide layer can decrease the wear rate. However, under severe wear conditions, the peeling of the oxide layer is also closely related to the shear stress. If the matrix becomes soft at a high temperature under a large shear stress, the oxide layer fractures when it reaches the critical thickness, accelerating the wear. This can be illustrated with the sample at 10 N: although the matrix had enough holding power to support the oxide layer, the oxide layer fractured and oxide particles appeared, causing an increase in the wear rate and friction coefficient.

Therefore, in order to have good wear resistance, the matrix needs to have sufficient strength at a high temperature. In addition to the thermal strength of the matrix, the toughness of the matrix also plays an important role with regard to wear resistance. Due to the high test temperature, severe oxidation occurs at the bumps of the contact surface. The contact bumps exhibit fast oxidation and high temperature, resulting in a thick oxide layer. Due to the large load on the bumps and internal stress of the oxide layer, the oxide layer peels off. In this case, a

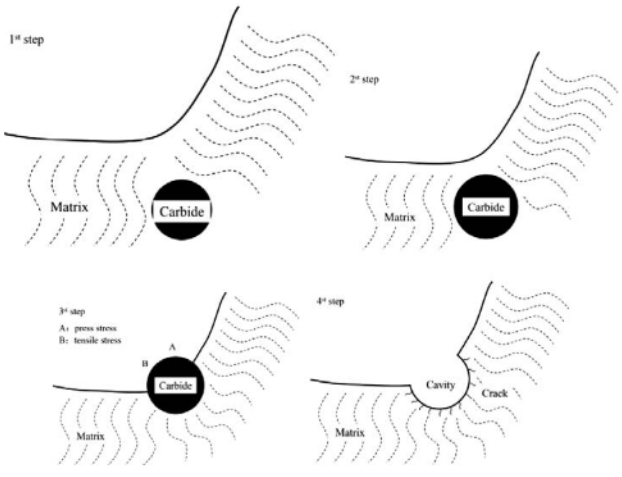

Figure 11: Schematic diagram of crack initiation

spalling of the oxide layer usually occurs at the contact surface, while the wear rate is hardly related to the toughness of the matrix. However, if there are coarse second phases in the matrix, the repeated friction force causes plastic deformation at the interface and forms a stress concentration. When the stress surpasses the critical bonding strength, the second phase peels off from the matrix, and a displacement difference between the matrix and the second phase occurs. Then cracks initiate, expend and fracture in the matrix, inducing a delamination of the oxide layer and increasing the wear rate. Therefore, if the matrix has the second phase, the initiation and growth of cracks depend on the toughness of the matrix. Besides, the composition and morphology of wear debris are directly related to the wear mechanism. Sullivan et al.[34] supposed the spalling of flaky oxides causes wear. So et al.[35] stated that fatigue causes the spalling of the oxide layer, which is only part of an entire oxide layer. Based on the tests, the oxide layer gradually peels off under loading, and the spalling of oxides accumulates and adheres to the formed oxide layer. The adhesion of oxides depends on the load and amount of spalling oxides. Besides, the adhesive oxides play an important role in reducing the wear.

Based on the effect of load on the wear characteristics at a high temperature, we suggest a diagram, shown in **Figure 12**. Under a low load, the oxides of the contact surface partly peel off and some fatigue cracks form in the oxide layer during the wear in the first step. An incomplete oxide layer results in the appearance of many oxide particles. Grooves are observed in the morphology due to particle sliding. The wear mechanism is typical abrasive-oxidative wear. In the second step, the load results in a deformation of the worn surface. The worn surface is covered with a loose oxide layer. The deformation and coarse carbides cause crack initiation in the matrix under the loading. The wear mechanism is transformed into oxidative wear. In the third step, the spalling oxide particles are tightly attached to the initial oxide layer, forming recompacted oxide regions under the high load.

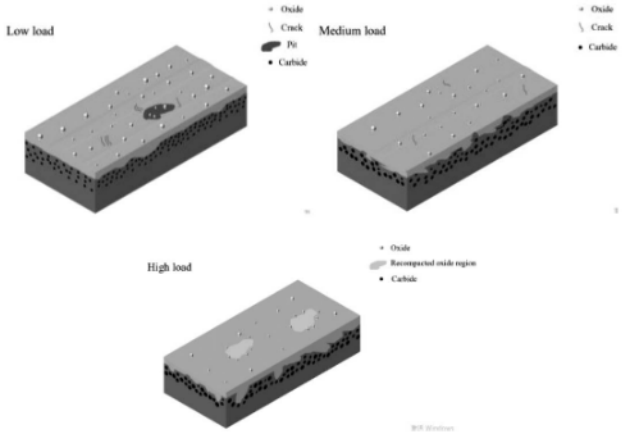

Figure 12: Physical model of wear characteristics under different loads

Small oxide particles scatter near the compacted oxide regions. In addition, carbides further coarsen and the oxide layer grows along the cracks. The wear mechanism transforms from oxidative wear to adhesive-oxidative wear.

5 CONCLUSIONS

In this work, the tribological performance of 5Cr5Mo2V steel under different loads was studied. The authors explained the reasons for the oxide-layer delamination and proposed a diagram. The following results were obtained:

1. As the load increases, the wear rate of 5Cr5Mo2V steel increases at 700 °C. The wear mechanism transformation is oxidative-abrasive wear → oxidative wear → adhesive-oxidative wear. Besides, the oxides on the worn surface are composed of FeO, Fe_2O_3 and Fe_3O_4.

2. The delamination of the oxide layer is attributed to the appearance of cracks in the matrix. Both the exfoliation of coarse carbides and displacement difference between the matrix and carbides induce crack initiation.

3. With the increase in the load, carbides are easier to coarsen. In addition, carbides transform from M_7C_3-type carbides to M_6C-type carbides at 700 °C. Coarse M_6C-type carbides cannot provide strong holding power and cause a high wear rate.

Acknowledgment

This work was carried out with the financial support from the National Key R&D Program of China (No. 2016YFB0300400 and 2016YFB0300402) and we gratefully acknowledge this support.

6 REFERENCES

[1] A. Yanagida, A. Azushima, Evaluation of coefficients of friction in hot stamping by hot flat drawing test, CIRP Annals – Manufacturing Technology, 58 (**2009**) 1, 247–250, doi:10.1016/j.cirp.2009.03.091

[2] A. Ghiotti, S. Bruschi, F. Medea, A. Hamasaiid, Tribological behavior of high thermal conductivity steels for hot stamping tools, Tribology International, 97 (**2016**), 412–422, doi:10.1016/j.triboint.2016.01.024

[3] C. Boher, S. Le Roux, L. Penazzi, C. Dessain, Experimental investigation of the tribological behavior and wear mechanisms of tool steel grades in hot stamping of a high-strength boron steel, Wear, (**2012**), 286–295, doi:10.1016/j.wear.2012.07.001

[4] K. Lange, L. Cser, M. Geiger, J. A. G. Kals, Tool Life and Tool Quality in Bulk Metal Forming, CIRP Annals, 41 (**1992**) 2, 667–675, doi:10.1016/s0007-8506(07)63253-3

[5] M. Wei, F Wang, S. Wang, X. Cui, Comparative research on the elevated-temperature wear resistance of a cast hot-working die steel, Materials and Design, 30 (**2009**) 9, 3608–3614, doi:10.1016/j.matdes.2009.02.023

[6] M. Wei, S. Wang, L. Wang, X. Cui, K. Chen, Effect of tempering conditions on wear resistance in various wear mechanisms of H13 steel, Tribology International, 44 (**2011**) 7–8, 898–905, doi:10.1016/j.triboint.2011.03.005

[7] Q. Li, J. Guo, A. Zhao, Effect of Upper Bainite on Wear Behaviour of High-Speed Wheel Steel, Tribology Letters, 67 (**2019**) 4, 121, doi:10.1007/s11249-019-1239-7

[8] D. Rai, B. Singh, J. Singh, Characterisation of wear behaviour of different microstructures in Ni–Cr–Mo–V steel, Wear, 263 (**2007**) 1, 821–829, doi:10.1016/j.wear.2006.12.014

[9] S. Li, X. Wu, X. Li, J. Li, X. He, Wear Characteristics of Mo-W-Type Hot-Work Steel at High Temperature, Tribology Letters, 64 (**2016**) 2, 1–12, doi:10.1007/s11249-016-0764-x

[10] S. Wang, F. Wang, X. Cui, K. Chen, Effect of secondary carbides on oxidation wear of the Cr–Mo–V cast steels, Materials Letters, 62 (**2008**) 2, 279–281, doi:10.1016/j.matlet.2007.05.018

[11] S. Li, X. Wu, S. Chen, J. Li, Wear Resistance of H13 and a New Hot-Work Die Steel at High Temperature, Journal of Materials Engineering and Performance, 25 (**2016**) 7, 2993–3006, doi:10.1007/s11665-016-2124-2

[12] N. Hashemi, A. Mertens, H.-M. Montrieux, J. T. Tchuindjang, O. Dedry, R. Carrus, J. Lecomte-Beckers, Oxidative wear behaviour of laser clad High Speed Steel thick deposits: Influence of sliding speed, carbide type and morphology, Surface and Coatings Technology, 315 (**2017**), 519–529, doi:10.1016/j.surfcoat.2017.02.071

[13] N. Ur Rahman, M. de Rooij, D. Matthews, G. Walmag, M. Sinnaeve, G. Römera, Wear characterization of multilayer laser cladded high speed steels, Tribology International, 130 (**2019**), 52–62, doi:10.1016/j.triboint.2018.08.019

[14] M. Pole, M. Sadeghilaridjani, J. Shittu, A. Ayyagari, S. Mukherjee, High temperature wear behavior of refractory high entropy alloys based on 4-5-6 elemental palette, Journal of Alloys and Compounds, 843 (**2020**), 156004, doi:10.1016/j.jallcom.2020.156004

[15] P. Jayashree, M. Bortolotti, S. Turani, G. Straffelini, High-Temperature Tribo-Oxidative Wear of a Cu-Based Metal-Matrix Composite Dry Sliding against Heat-Treated Steel, Tribology Letters, 67 (**2019**) 4, 110, doi:10.1007/s11249-019-1227-y

[16] H. Tang, H. Zhang, L. Chen, S. Guo, Novel laser rapidly solidified medium-entropy high speed steel coatings with enhanced hot wear resistance, Journal of Alloys and Compounds, 772 (**2018**), 719–727, doi:10.1016/j.jallcom.2018.09.122

[17] G. A. Fontalvo, C. Mitterer, The effect of oxide-forming alloying elements on the high temperature wear of a hot work steel, Wear, 258 (**2005**) 10, 1491–1499, doi:10.1016/j.wear.2004.04.014

[18] Y. Wang, L. Zhang, T. Wang, X. D. Hui, W. Chen, C. F. Feng, Effect of sliding velocity on the transition of wear mechanism in $(Zr,Cu)_{95}Al_5$ bulk metallic glass, Tribology International, 101 (**2016**), 141–151, doi:10.1016/j.triboint.2015.11.012

[19] Y. Shi, X. Wu, Research on Oxidation Wear Behavior of a New Hot Forging Die Steel, Journal of Materials Engineering and Performance, 27 (**2017**) 1, 176–185, doi:10.1007/s11665-017-3078-8

[20] Y. Qian, M. Li, Y. Zhang, Effect of External Stress on the Selective Oxidation of Ti_3Al Base Alloy at 500-700 °C, Acta Metallrugica Sinica, 39 (**2003**), 989–994

[21] X. Cui, S. Wang, Q. Jiang, B. Hong, High-Temperature Wear Mechanism of Cast Hot-Forging Die Steel 4Cr3Mo2NiV, Acta Metallrugica Sinica, 41 (**2005**), 1116–1120

[22] M. J. Santofimia, L. Zhao, J. Sietsma, Model for the interaction between interface migration and carbon diffusion during annealing of martensite-austenite microstructures in steels, Scripta Materialia, 59 (**2008**) 2, 159–162, doi:10.1016/j.scriptamat.2008.02.045

[23] V. V. Popov, Diffusion Parameters of Carbide-Forming Elements in Fe-M-C Systems, Defect and Diffusion Forum, 283–286 (**2009**), 687–696, doi:10.4028/www.scientific.net/ddf.283-286.687

[24] S. Z. Yang, N. Li, Y. H. Wen, H. B. Peng, Effect of ageing temperature after tensile pre deformation on shape memory effect and precipitation process of $Cr_{23}C_6$ carbide in a FeMnSiCrNiC alloy, Materials Science and Engineering: A, 529 (**2011**), 201–206, doi:10.1016/j.msea.2011.09.018

[25] D. Wu, F. Wang, J. Cheng, C. Li, Effects of Nb and Tempering Time on Carbide Precipitation Behavior and Mechanical Properties of Cr-Mo-V Steel for Brake Discs, Steel Research International, 89 (**2018**) 5, 1700491, doi:10.1002/srin.201700491

[26] J. Guo, H. Qu, L. Liu, Y. Sun, Y. Zhang, Q. Yang, Study on stable and meta-stable carbides in a high speed steel for rollers during tempering processes, International Journal of Minerals, Metallurgy and Materials, 20 (**2013**) 2, 146–151, doi:10.1007/s12613-013-0706-7

[27] X. H. Cui, S. Q. Wang, F. Wang, K. M. Chen, Research on oxidation wear mechanism of the cast steels, Wear, 265 (**2008**) 3–4, 468–476, doi:10.1016/j.wear.2007.11.015

[28] M. Shen, Y. Zhou, C. Song, J. Mo, M. Zhu, Local Fatigue Behavior of 7075 Alloy under Condition of Rotational Fretting Wear, Journal of Aeronautical Materials, 33 (**2013**) 2, 46–50

[29] J. R. Fleming, N. P. Suh, Mechanics of crack propagation in delamination wear, Wear, 44 (**1977**) 1, 39–56, doi:10.1016/0043-1648(77)90083-7

[30] S. Jahanmir, N. P. Suh, Mechanics of subsurface void nucleation in delamination wear, Wear, 44 (**1977**) 1, 17–38, doi:10.1016/0043-1648(77)90082-5

[31] T. F. J. Quinn, D. M. Rowson, J. L. Sullivan, Application of the oxidational theory of mild wear to the sliding wear of low alloy steel, Wear, 65 (**1980**) 1, 1–20, doi:10.1016/0043-1648(80)90002-2

[32] T. F. J. Quinn, Review of oxidational wear, Tribology International, 16 (**1983**) 5, 257–271, doi:10.1016/0301-679x(83)90086-5

[33] T. F. J. Quinn, Review of oxidational wear Part II: Recent developments and future trends in oxidational wear research, Tribology International, 16 (**1983**) 5, 305–315, doi:10.1016/0301-679x(83)90039-7

[34] J. L. Sullivan, S. S. Athwal, Mild wear of a low alloy steel at temperatures up to 500 °C, Tribology International, 16 (**1983**) 3, 123–131, doi:10.1016/0301-679x(83)90053-1

[35] H. So, The mechanism of oxidational wear, Wear, 184 (**1995**) 2, 161–167, doi:10.1016/0043-1648(94)06569-1